J Appl Phycol (2016) 28:803–812
DOI 10.1007/s10811-015-0652-z

Impact of nitrogen limitation on biomass, photosynthesis, and lipid accumulation in *Chlorella sorokiniana*

Sangeeta Negi[1] · Amanda N. Barry[2] · Natalia Friedland[1] · Nilusha Sudasinghe[3] · Sowmya Subramanian[1] · Shayani Pieris[4] · F. Omar Holguin[3] · Barry Dungan[3] · Tanner Schaub[3] · Richard Sayre[1,2]

Received: 22 December 2014 / Revised and accepted: 21 June 2015 / Published online: 8 July 2015

Abstract Induction of oil accumulation in algae for biofuel production is often achieved by withholding nitrogen. However, withholding nitrogen often reduces total biomass yield. In this report, it is demonstrated that *Chlorella sorokiniana* will not only accumulate substantial quantities of neutral lipids when grown in the absence of nitrogen but will also exhibit unimpeded growth rates for up to 2 weeks. To determine the physiological basis for the observed increase in oil and biomass accumulation, we compared photosynthetic and respiration rates and chlorophyll, lipid, and total energy content under ammonia replete and deplete conditions. Under N-depleted growth conditions, there was a 64 % increase in total energy density and a ~20-fold increase in oil accumulation relative to N-replete growth leading to a 1.6-fold greater total energy yield in N-depleted than in N-replete cultures. We propose that the higher energy accumulation in N-depleted cultures is due to enhanced photosynthetic energy capture and conversion associated with reduced chlorophyll levels and reduced self-shading as well as a shift in metabolism leading to the accumulation of oils.

Keywords Microalgae · *Chlorella sorokiniana* · Photobioreactor · Lipid production · Biofuels · Photosynthesis

Sangeeta Negi and Amanda N. Barry shared first author

Electronic supplementary material The online version of this article (doi:10.1007/s10811-015-0652-z) contains supplementary material, which is available to authorized users.

✉ Richard Sayre
rsayre@newmexicoconsortium.org

[1] New Mexico Consortium, Los Alamos, NM 87544, USA

[2] Bioscience Division, Los Alamos National Laboratory, Los Alamos, NM 87545, USA

[3] Center for Animal Health, Food Safety & Bio-Security, New Mexico State University, Las Cruces, NM 88003, USA

[4] Department of Biology, Missouri Baptist University, Saint Louis, MO 63141, USA

Introduction

With the continuing depletion of fossil fuels around the globe and the need to reduce greenhouse gas emissions, efforts to find alternative and renewable fuel sources are underway. Biomass production systems are an appealing substitute for fossil fuels, due to their reduced environmental impact and carbon dioxide emissions. Microalgae are an attractive alternative to terrestrial crops due to the potential for longer growing seasons and reduced competition with food production. Furthermore, by utilizing waste water or effluent, microalgae production in pond systems can facilitate water and nutrient recycling. Microalgae also have the capability of producing substantial biomass (10–40 g DW m^{-2} day^{-1}) per unit land area, producing as much as twofold to tenfold greater biomass than terrestrial systems (Sayre 2010; Subramanian et al. 2013). Given the tremendous biodiversity of algae and the fact that few species have been investigated for the production potential, there undoubtedly remains great potential for the discovery of enhanced biofuel production strains (Mata et al. 2010).

To increase triacylglycerol (TAG) accumulation or the energy density of algal biomass, nitrogen (N) limitation or starvation has frequently been utilized (Breuer et al. 2012). During N starvation, it is thought that there is a rechanneling of reduced carbon or remodeling of existing lipids leading to the accumulation of triglycerides (Breuer et al. 2012). While lipid droplets, cell volume, carotenoid, and carbohydrate content

increase during N starvation in green algae, in general cell division ceases associated with reduced protein, chlorophyll, and total biomass levels (Cakmak et al. 2012).

Recently, a promising strain of microalgae, *Chlorella sorokiniana*, has been shown to have a high lipid content under a wide range of environmental growth conditions (Li et al. 2013). Growth in a bioreactor using mixo- and/or heterotrophic media supplemented with glucose enabled *C. sorokiniana* UTEX 1230 to accumulate 30–40 % of its cell mass as lipids (Rosenberg et al. 2014). *C. sorokiniana* has also been shown to reduce carbon monoxide, carbon dioxide, and nitrogen oxide emissions from wastewater (Lizzul et al. 2014). Under N-starvation, *C. sorokiniana* was shown to accumulate greater levels of neutral lipids than when grown under N-replete conditions but exhibited an increased damage to photosystem II (PSII) potentially reducing total biomass and energy yields (Zhang et al. 2013).

To fully examine the potential of *C. sorokiniana* as a biofuel source, we measured a variety of phenomic parameters for cultures grown in environmentally controlled photobioreactors (ePBRs) that simulate a production pond environment in depth, light, and turbidity. These ePBRs have been shown to be a useful tool for examining cell growth and lipid production for *Nannochloropsis oculata* under various growth regimes (Tamburic et al. 2014). Comparative growth, biomass, photosynthesis, respiration rates, and lipid productivity analyses of *C. sorokiniana* grown in the presence and absence of N demonstrate that this species has the potential to produce greater total energy yield when grown under N-limiting conditions than when grown under N-replete conditions. This increased energy yield is attributed to two factors, a shift in the accumulation of energy storage products favoring lipid accumulation and to increased light penetration into the culture supporting greater total biomass yields.

Materials and methods

Chlorella sorokiniana strain KAN1228, a genetically homogenous culture isolated from single colony from strain UTEX 1230, was obtained from Phycal Inc. (St. Louis, MO, USA) and maintained on Sueoka's high salt (HS) plates and liquid media (Sueoka 1960). This medium utilizes ammonium chloride (9.35 mM) as the sole nitrogen source with no supplemental carbon for phototrophic growth.

Photobioreactor cultures

In order to determine appropriate sampling times for large scale experiments, a trial experiment was first run. A 25-mL starter culture in HS medium was grown to 1.7×10^7 cells mL^{-1} and inoculated into three 550 mL photobioreactors (Phenometrics; ePBRs; Supplemental Figure 1) at a 1:100 dilution. Lights on the ePBRs were calibrated and programmed to provide a 12-h sinusoidal light cycle with a peak intensity at noon of 2,000 μmol photons m^{-2} s^{-1} (Supplemental Figure 1). Temperature was a constant 25 °C, and ePBRs were stirred with a magnetic stir bar at 200 rpm. Filtered air was bubbled constantly through the growing cultures from the bottom up. Culture density (OD_{750}) was measured daily on a UV/Vis spectrophotometer and 1 mL samples were taken for Nile red staining for lipids and cell counts by flow cytometry. After cells reached stationary phase, they were harvested by centrifugation in sterile 500 mL centrifuge tubes at 18,600× *g* for 15 min, and resuspended in HS medium for growth without nitrogen (NH_4Cl) after washing with the same medium. The results of the phenomics assay described below were used to design the large scale experimental system.

For the large scale experiments, a 25-mL starter culture of *C. sorokiniana* was used to inoculate a 150-mL culture (1:100 dilution) in N-containing HS medium and grown to a cell density of 1.6×10^7 cells mL^{-1}. Eighteen ePBRs, each a total volume of 550 mL, were inoculated with 5.5 of the 150 mL starter cultures. On day 14 (14 days after start), the contents (~500 mL) of the ePBRs were centrifuged in sterile centrifuge tubes, and the pellet was resuspended in HS medium with or without nitrogen (NH_4Cl). All experiments were done in triplicate for each time point and each treatment.

Cell harvesting and biomass estimation

On day 7 (7 days after start), day 14, day 19, and day 29, the total contents of the individual ePBRs were harvested. Cells were collected by centrifugation at 18,600×*g* for 15 min. Cell pellets were frozen immediately in liquid N_2 and later freeze-dried using a Flexi-Dry microprocessor controlled lyophilizer. After drying, pellets were weighed for total biomass. Total volume of cultures before centrifugation was measured for all harvested ePBRs. At each time point, OD_{750} was measured for cell density.

Nile red lipid staining and flow cytometry

At each time point, 1 mL of suspended cells was used to determine cell counts and Nile red staining for lipid content by flow cytometry. For flow cytometry measurements, 10 μL of Nile Red (1 mg L^{-1}) was added to 750 μL of cells. Cells were vortexed for 5 s at maximum speed in bench top vortexer. Subsequently, 200 μL of sample was added to each of three wells in a 96-well plate and cell counts and Nile Red staining cells were counted in an Accuri flow cytometer. The Nile Red fluorescence intensity at 585 nm was detected using an excitation wavelength of 488 nm.

Chlorophyll (Chl) fluorescence induction measurements

For Chl fluorescence induction analyses, cell suspensions of *C. sorokiniana* were adjusted to yield a Chl concentration of ~2.5 μg Chl mL^{-1} and placed in a kinetic fluorometer (FL-3500, Photon Systems Instruments). Following dark adaptation, Chl fluorescence was induced using an actinic flash of 100 μs. Chl fluorescence is normalized to the maximum Chl fluorescence yield when the reaction centers are closed (Perrine et al. 2012).

Photosynthetic oxygen evolution as a function of light intensity

The CO_2-dependent rates of oxygen evolution were assayed using a Clark-type oxygen electrode (Hansatech Instruments). Cells were adjusted to a Chl concentration of 15 μg Chl mL^{-1} in 20 mM HEPES buffer (pH 7.4). Rates of oxygen evolution were measured as a function of increasing light intensity (650 nm wavelength red light). The photon flux density used for oxygen evolution measurements was 450 μmol photons m^{-2} s^{-1} of red light. Significantly, at the chlorophyll concentrations and light intensity used in the oxygen electrode, there was no impairment in maximal rates of photosynthesis due to self-shading. The same experiment was repeated in the presence of saturating amounts (10 mM) of $NaHCO_3$.

Chlorophyll quantification

For Chl quantification, 1 mL of *C. sorokiniana* cell suspension was spun down and the supernatant was replaced by 1 mL of 100 % methanol. After resuspending in methanol, cells were incubated in the dark for 15 min, repelleted, and the Chl was measured spectrophotometrically according to Mackinney's method (Mackinney 1941).

Calorific analysis

Calorific value of *C. sorokiniana* biomass was determined using a Parr 6300 bomb calorimeter (Parr Instrument Company, USA). Dried algal cells (approximately 25 mg per sample) were combusted to estimate the calorific energy value of samples per gram dry weight. Benzoic acid tablets were used to calibrate the calorimeter and mineral oil (450 μL) was used as a spike for combustion of algal cells. These assays were done in triplicate and mean values and standard error was calculated.

FAME quantitation by GC/MS and lipid analysis by FT-ICR mass spectrometry

Lipid extraction was performed according to Folch et al. (1957). Lyophilized algal samples were extracted with 2:1 chloroform: methanol mixture (*v/v*) containing 5 mM (15:0/15:0) phosphatidylethanolamine (PE; Avanti Polar Lipids, USA CAT#850704P) as the internal standard. For extraction, 20 μL of this solution was added to 1 mg of dry tissue and the mixture was vortexed thoroughly. Extracts were centrifuged and the supernatant was carefully removed without disturbing the pellet. Extraction was repeated by adding 2:1 chloroform: methanol mixture containing no internal standard at the same ratio (i.e., 20 μL solution to 1 mg of initial dry tissue mass). The supernatants were combined and stored at −20 °C until analysis by both GC/MS (fatty acid methyl ester quantification, FAME) and FT-ICR MS.

Lipid and fatty acid analysis

Base catalyzed FAME analysis was performed for each Folch extract. Briefly, 15 μL of extract was added to 100 mL of 0.2 N KOH in MeOH in a 250-μL GC vial insert. Samples were then placed in a hot water bath at 50 °C for 30 min. Next, 50 μL of 1 M glacial acetic acid was added to quench the reaction and samples were back extracted with 50 μL hexane that contained internal standard (C23:0, methyl tritridecanoate) for GC/MS analysis. A Hewlett Packard 5890 GC with a 5972a MSD was used to detect FAMEs from 2 μL injections onto a J&W DB 23 column (30 m×0.25 mm diam×.25 μm film, Agilent, USA) with helium as the carrier gas. The initial oven temperature was 80 °C and ramped 20 °C min^{-1} to 220 °C and held for 6 min. A standard spectra tune was performed and samples were quantified using internal standard calibration (37 component FAME mix, Sigma-Aldrich, USA).

Dilute lipid extracts were analyzed by direct infusion electrospray ionization Fourier transform-ion cyclotron resonance mass spectrometry (FT-ICR MS) as recently described (Holguin and Schaub 2013). For the positive ion mode FT-ICR MS analysis, algal lipid extracts were diluted 200-fold in 1:2:4 chloroform to methanol to 2-propanol containing 0.1 mM aqueous sodium acetate ratio. For negative ion mode, lipid extracts were diluted 20-fold in 1:2:4 chloroform to methanol to 2-propanol containing 0.5 mM ammonium hydroxide ratio. All diluted algal lipid extracts were filtered through Acrodisc CR 13 mm syringe filters with 0.2 μm PTFE membrane (Pall Corporation, USA) to remove any suspended particulate matter prior to analysis.

FT-ICR MS analyses were performed in both positive and negative ionization modes. Ultra high mass resolving power (m/Δm50 %>400,000) and sub-part-per-million mass accuracy of FT-ICR-MS combined with Kendrick mass sorting allow unique elemental composition assignments to each mass spectral peak. The assigned elemental compositions and heteroatom classes were identified as a given lipid class by searching against a list of lipids using an in-house built Microsoft Excel macro. Because suitable analytical standards

are not available for even a fraction of the observed compounds, response factors are not applied and abundance information for each observed mass spectral signal is reported on a relative basis where mass spectral signal-to-noise ratios are normalized to that of a PE (15:0/15:0) internal standard. Within the constraints of this detailed qualitative analysis, abundance information may be compared for a particular compound (or compound class) between samples but not between compound classes within the same sample.

Results and discussion

Cell growth in photobioreactors

One of the challenges when comparing the relative productivity, lipid, and energy yield of various algae strains is the broad range of dissimilar environmental conditions under which they are grown. Furthermore, many laboratory growth systems bear little resemblance to ponds in which algae are grown at large scale. The culture depth, mixing rates, temperature, light fluctuations, nutrient content, etc., can impact biomass yield and energy density of the harvested biomass. In addition, it is a common practice to increase the lipid content or energy density of the biomass by withholding a macro-nutrient such as N or P. Recently, the National Alliance for Advanced Biofuels and Bioproducts (NAABB) reported in a survey of over 1,000 independent algal isolates that the green alga *C. sorokiniana* had great potential both for biomass and lipid production under laboratory growth conditions. In this study, we have investigated the growth of *C. sorokiniana* in ePBRs that simulate pond-like environments (depth, vertical illumination, light fluctuation, and nutrients) with the exception that we held the temperature constant. We have compared growth following the removal of N to determine the impact of N withholding on cell physiology, lipid accumulation, biomass productivity, and energy density. To preliminarily assess potential biomass and lipid production, we carried out an exploratory growth trial over several weeks in which *C. sorokiniana* was grown photoautotrophically in the presence and absence of N in ePBRs. Cell numbers and oil accumulation were monitored (Supplemental Figure 2). Using a low inoculation cell density, we observed that cultures achieved mid-log phase growth at day 14. At this time point, we exchanged the growth media of the cultures to media lacking ammonium (−N) and followed their growth rates and relative lipid contents in comparison to a control. Unexpectedly, we observed that rapidly growing cells switched to media lacking ammonia maintained growth rates similar to those grown with ammonia for an additional 2 weeks. Furthermore, cells grown in the absence of N accumulated increased levels of neutral lipids. Based on these preliminary trials, we expanded the trials for growth in ePBRs and assessed cellular respiration rates, photosynthetic parameters, lipid content and composition, biomass yield, and energy density.

Cell density and biomass composition

To understand the effects of N deprivation on growth and biomass accumulation, we monitored changes in cell numbers and dry weight accumulation over several weeks. From day 7 to day 14 following inoculation, cells grown in N-replete media had a 3.3, 4.3, and 3.6-fold increase in light scattering, total cell numbers, and biomass accumulation, respectively (Fig. 1). During this growth period, however, the biomass per cell decreased 16 % from 12.7 to 10.7 ng cell^{-1} potentially reflecting a change in carbohydrate (density=1.56 g cm^{-3}) to lipid ratio (density=0.91 g cm^{-3}). After 14 days of cultivation, the total culture volume was pelleted, washed, and the media was exchanged with N-replete or N-deplete media. Due to the unavoidable loss of cells during media replacement by centrifugation, the OD_{750}, cell numbers, and biomass were slightly lower on day 18 than on day 14 (Fig. 1a–c). Surprisingly, during the 2 weeks following media exchange total biomass increased by the same extent (4.5-fold) in cultures grown with or without N. These results indicate that *C. sorokiniana* is capable of robust growth under N-limiting conditions. These results suggest that the cultures grown in the absence of N have sufficient N-reserves for extended periods of growth. Although N starvation under photoautotrophic growth conditions can result in increased lipid production, many algal strains exhibit slower growth rates in the absence of N, leading to lower overall biomass and energy yields (Huerlimann et al. 2010). Some species (*C. minutissima)*, however, are capable of high rates of growth in the absence of N, equivalent to those in N-replete media (Tang et al. 2011). This high growth rate in N-deplete media is thought to result from the utilization of stored N reserves rather than from the utilization of N harvested from salvage pathways associated with the turnover of proteins which would be expected to ultimately impair growth (Lourenco and Barbarino 1998). In addition, the redox state of the N available in the media may impact growth rates. In previous studies, *C. sorokiniana* was shown to grow faster with urea and ammonium than with nitrate (Ramanna et al. 2014; Lizzul et al. 2014). This is not surprising since the utilization of ammonium or reduced nitrogen (urea) requires less energy than nitrate (more oxidized) for amino acid synthesis. To our knowledge, however, this is the longest period of sustained high growth in the absence of N relative to growth in N-replete media observed for any algal species.

Chlorophyll content and chlorophyll fluorescence kinetics

N-starvation in algae is known to result in reduced protein and Chl content (Breuer et al. 2012; Lv et al. 2010;

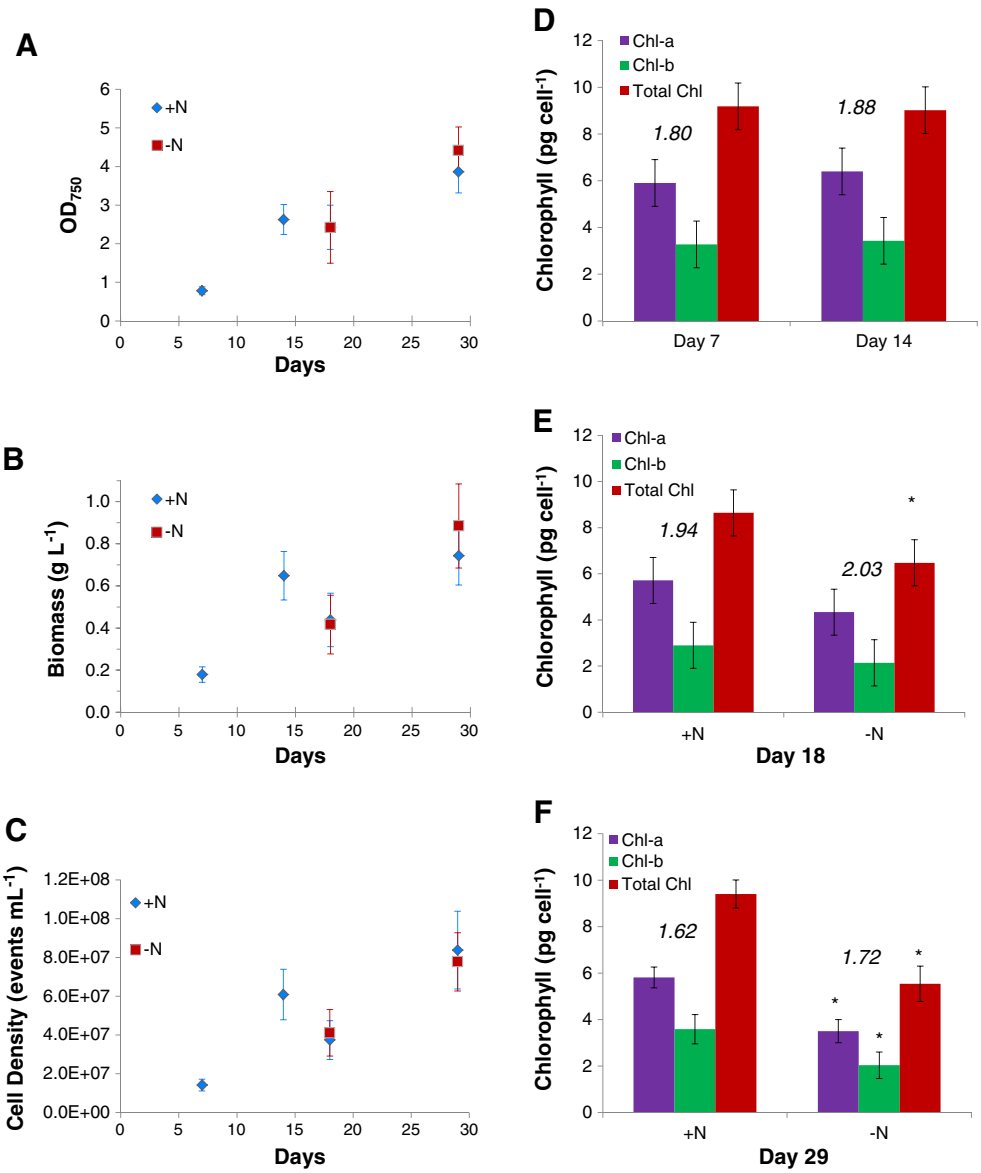

Fig. 1 Growth rates, biomass, cell number, and chlorophyll content of cells grown on plus and minus nitrogen media. **a** Photoautotrophic growth of cells grown in +N and −N media. **b** Dry cell biomass of cells grown in N-replete and N-deplete media. **c** Cell number in N-replete and N-deplete media. **d** Chl content per cell in N-replete grown cells on day 7 and day 14. **e** Chl content per cell in N-replete and N-deplete grown cells on day 18. **f** Chl content per cell in N-replete and N-deplete grown cells on day 29. Results represent the average and SE of three independent measurements. Chl *a*/*b* ratio in *italics*

Pruvost et al. 2011), often resulting in a "degreening" of cells. The most significant changes in cell ultrastructure following N-starvation are changes in the chloroplast structure associated with alterations in thylakoid membrane structure and degradation of plastidial membrane lipids indicating that the photosynthetic apparatus is particularly sensitive to N depletion (Siaut et al. 2011; Wang et al. 2011). Impairment in photosynthesis can also accelerate photodamage under high light conditions associated with the production of reactive oxygen species (ROS). Significantly, *C. sorokiniana* and other microalgae have been shown to accumulate higher levels of carotenoids under N-starvation and high light conditions than under N-replete conditions including the carotenoids lutein, astaxanthin, and β-carotene, which are known to quench ROS (Sayed and Hegazy 1992). To determine whether the photosynthetic apparatus was altered by N-depletion, the Chl content per cell was compared in cultures grown with and withoutnitrogen. Cultures grown in N-replete media had very similar total cellular Chl contents on days 7, 14, 18, and 29 (Fig. 1d–f). After N depletion, however, total cellular Chl decreased 24 and 40 % relative to N-replete cultures 4 days and 2 weeks after N-removal, respectively (Fig. 1e and f). Interestingly, Chl *a*/*b* ratios remained unchanged up to day 18 in N deplete media. However, the Chl *a*/*b* ratio was ~16 % lower in both N-replete and N-deplete conditions on day 29 compared to day 18 suggesting an increase in light harvesting antenna size (Fig. 1e,f; Perrine et al. 2012; Zhang et al. 2013).

Chlorophyll fluorescence kinetic measurements are commonly used to analyze photosystem II function. As previously shown, Chl fluorescence kinetics and photosystem II (PSII)

photochemistry are often impacted by N depletion in algal cultures (Sayed and Hegazy 1992; Simionato et al. 2013). Growth of algae in N-deplete media has previously been shown to result in reduced capacity to reduce plastoquinone at the PSII Q_B site, reduced numbers of active PSII reaction centers, and increased non-photochemical quenching (Berges et al. 1996; Lu et al. 2001). To determine if there was an alteration in energy capture and conversion efficiency, Chl fluorescence rise kinetics were measured. No difference in the Chl fluorescence rise kinetics was observed between day 7 and day 14 for cultures grown in N-replete media (Supplemental Figure 3A). Notably, on day 29, N-depleted cells exhibited faster chlorophyll fluorescence rise kinetics compared to N-sufficient cells suggesting that N-depleted cells may have reduced PSII electron acceptor pool sizes, or impairments in the ability to turnover reduced plastohydroquinone (PQH_2; Supplemental Figure 3B, C).

Growth media associated changes in overall PSII quantum efficiency were also determined by measuring the ratio of variable (F_v) to maximal (F_m) Chl fluorescence yield (Table 1). On day 7 and day 14, cells grown in N-replete media exhibited high PSII quantum efficiencies (F_v/F_m= 0.83 to 0.80, respectively). After medium exchange to N-deplete medium on day 18, cells did not show any change in PSII quantum efficiency, whereas on day 29, N-depleted cells showed a decrease in quantum efficiency compared to N-replete cells from 0.74 to 0.62, respectively. These results indicated that reductions in PSII photochemical efficiency under N-starvation occurred only after a long period of growth in N-deplete medium.

Photosynthesis and respiration

To determine the effects of N-replete and N-deplete media on photosynthesis, CO_2-dependent rates of oxygen evolution were measured using whole cells in air and in saturating concentrations of bicarbonate. Photosynthetic rates in cells grown in N-containing medium decreased 38 % from day 7 to 14 per Chl (Figs. 1 and 2). After medium exchange, cells grown in N-deplete media had a 22 % lower maximum photosynthesis rate (in the presence of bicarbonate) compared to cells grown in N-replete medium on day 18. On day 29, the photosynthetic rates of cells grown in N-replete medium was 34 % higher than cells grown in N-deplete medium measured in the presence of bicarbonate. In air, the maximum photosynthesis rate for cells grown in N-deplete medium was 23 % lower than cells grown in N-replete medium on day 18 and 41 % lower on day 29. These differences in photosynthetic rates were further exacerbated at the cellular level by the substantial loss in Chl content per cell in N-depleted cultures (Fig. 1e and f). At days 18 and 29, there was a 25 and 41 % reduction, respectively, in Chl content per cell for cultures grown in the absence of N relative to those grown with N. These results are consistent

Table 1 PSII apparent quantum efficiency (F_v/F_m) of cells grown with and without nitrogen

Days cultured	F_v/F_m +N	F_v/F_m −N
7	0.83	–
14	0.80	–
18	0.81	0.79
29	0.74	0.62

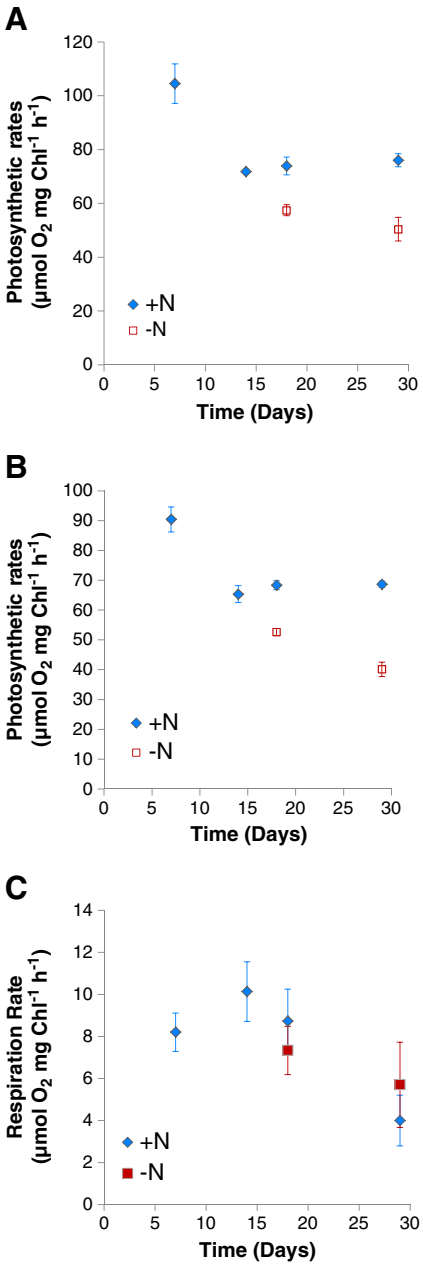

Fig. 2 Photosynthetic oxygen evolution and respiration rates in nitrogen-replete (+N) and nitrogen-deplete (−N) cells. Net photosynthesis rates were measured in **a** the absence of $NaHCO_3$ or **b** presence of 10 mM $NaHCO_3$ at 450 µmol photons m^{-2} s^{-1}. **c** Dark respiration rates. Results represent the average and SE of three independent measurements

with other findings that photosynthetic rates are substantially reduced in algal cultures grown under N-deplete conditions (Siaut et al. 2011; Simionato et al. 2013). To account for the similar biomass and cell numbers (Fig. 1b, c) for cultures grown with and without N, however, we need to consider the impact of light penetration in the ePBRs used in this experiment (20 cm). In actively mixed ePBRs, much like in ponds, there is a sharp decrease in available light intensity away from the surface due to absorption by the photosynthetic pigments as well as by light scatter (Carvalho et al. 2011). Photosynthesis occurs mostly in cells near the culture surface, whereas the mutual shading of cells causes steep reductions in light intensity with depth (Neidhardt et al. 1998; Murphy and Berberoglu 2012). In N-replete cultures, photosynthesis light saturates at 1/4 full sunlight intensity and light penetration is substantially reduced at high culture densities due to self-shading (Perrine et al. 2012). Assuming that light scattering is similar in N-replete and N-deplete cultures having nearly identical cell numbers per mL then it would be anticipated that the degree of light penetration with depth would be similar in both cultures if the Chl density was identical. Alternatively, if the there were differences in Chl concentrations per mL between the cultures then there would be more (low Chl density) or less (high Chl density) light penetration with depth (Fig. 3). Since N-deplete cultures had substantially reduced Chl content per cell relative to N-replete cultures we can assume that N-deplete cultures experienced less shading and deeper light penetration compared to N-replete cultures. These conclusions are consistent with algal mutants where antenna size has been reduced which also show that increased growth is attributed to reduction in Chl per cell rather than from alterations in Chl *a/b* ratios associated with changes in the size of the peripheral light harvesting complex (Perrine et al. 2012).

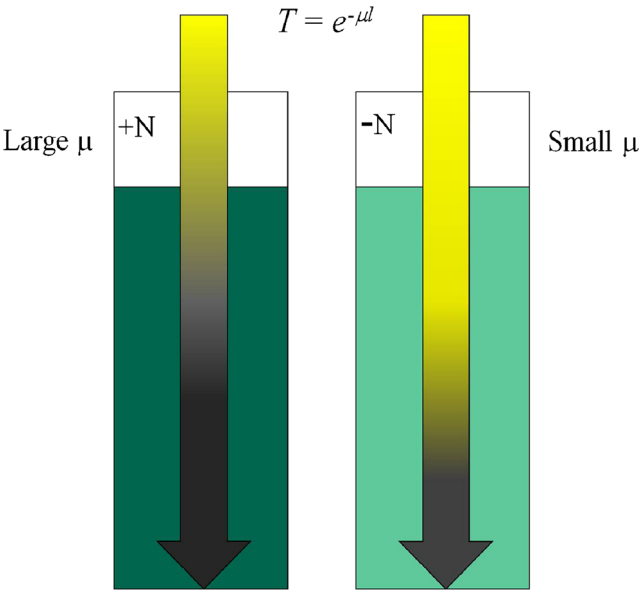

Fig. 3 Model of light penetration in the ePBRs. The Lambert's Law equation is listed where T=transmittance, μ=attenuation coefficient, and l=light path length. A smaller μ corresponds to a larger l value if T is held constant

Previous studies with *C. sorokiniana* C3 grown in the absence of N demonstrated, a substantial drop in PSII quantum efficiency (F_v/F_m) from 0.7 to 0.15 even when grown under low light (70 μmol photons m^{-2} s^{-1}) conditions in flasks over an 8-day period (Zhang et al. 2013). In the current study, the PSII quantum efficiency (F_v/F_m) dropped only marginally from 0.83 to 0.62 (Table 1). It is not apparent why there were differences in PSII quantum efficiency between the two studies, however, growth conditions and N depletion strategies were dissimilar between the two studies.

In contrast to photosynthetic traits, there was no significant difference in respiration rates when expressed on a Chl basis between cells grown in N-replete or N-deplete cultures over time, although respiration rates did decrease with culture age in both treatments (Fig. 2c). On a per cell basis, however, N-deplete cultures had 2-fold lower respiration rates on day 29 than did N-replete cells. Regardless, the magnitude of changes in the respiration rates were substantially less than the changes in net photosynthesis rates.

Lipid and energy density

Many studies have shown increased lipid accumulation in microalgae after N-starvation or under other nutrient stress conditions (Cakmak et al. 2012; Li et al. 2013; Siaut et al. 2011). The algal species *Chlorella* sp. UTEX 2219-4 was shown to accumulate starch granules as well as oil bodies after three days of N-starvation, resulting in an increase in total biomass and energy yield (Wang et al. 2011). Several studies have shown that stress conditions that enhance oil accumulation also reduce growth rates, perhaps due to substantial lipid remodeling or stress-induced growth impairment (Sharma et al. 2012; Spolaore et al. 2006).

Direct-infusion FT-ICR mass spectrometry (FT-ICR MS) was performed to monitor qualitatively the lipid compositional changes that occurred during growth with the different treatments (Holguin and Schaub 2013). Lipid-associated mass spectral peaks at ~1,300 and ~1,100 were observed for positive and negative ion mode FT-ICR mass spectra, respectively. Following elemental composition assignment, signals that correspond to ^{13}C and other heavy nuclide-containing compounds are removed, and mono-isotopic compounds were grouped by lipid class. The relative distribution of the six most abundant lipid classes observed by FT-ICR MS is shown in Table 2. A 20-fold increase in TAG signal was observed for N-depleted cells at day 29 relative to day 7. In contrast, there was no increase in TAG content observed for cultures grown in N-replete media even after 29 days. We observed nearly identical results by Nile Red staining for lipids (Supplemental Figure 5). Similarly, increases in diacylglycerols were only observed in N-depleted cultures

Table 2 FT-ICR MS derived lipid class analysis for the most abundant observed lipid classes

Lipid class	Fold change/dry weight (data are relative to values on day 7)	
	29 days −N	29 days +N
PG	−0.15 (±0.03)	1.09 (±0.45)
SQDG	−0.42 (±0.03)	−0.69 (±0.11)
TAG	20.09 (±2.06)	−0.53 (±0.15)
PC	−0.93 (±0.08)	−0.60 (±0.05)
DGDG	1.66 (±0.01)	1.22 (±0.23)
PE	−0.74 (±0.09)	−0.57 (±0.03)

Peak magnitudes for individual lipids were scaled to that of an internal standard, grouped according to lipid class and summed. Fold change for each lipid class was calculated relative to day 7. Reductions in lipid levels relative to levels on day 7 are indicated by negative values. Error values derive from sampling, harvesting, sample preparation, and FT-ICR MS measurement of three biological replicates (isolated/replicated cultures)

DGDG digalactosyldiglyceride, *PC* phosphatidylcholine, *PE* phosphatidylethanolamine, *PG* phosphatidylglycerol, *SQDG* sulfoquinovosyl diacylglycerol

after 29 days growth. This is consistent with what was observed in preliminary trial experiments by Nile Red lipid staining (Supplemental Figure 2). For N-replete culture, SQDG content decreased two-fold between day 14 and day 18 before increasing again on day 29. For N-deplete cultures, SQDG content decreased monotonically throughout the growth period to yield a 0.42-fold decrease in relative abundance between day 7 and day 29. Similar to SQDG, higher phosphatidylcholine (PC) content was observed for the N-replete cultures than the N-deplete cultures on day 29. Because SQDG is a structural component of the thylakoid membrane, it is inferred that increased N availability facilitated chloroplast growth/synthesis for this late growth period sample (which is reflected by the photosynthetic rates enumerated above) but its reduction under N-deplete growth conditions may have contributed to the reduced photosynthesis in these cultures over time. Interestingly, another chloroplast thylakoid-specific lipid had the opposite trends in abundance relative to SQDG over time. Total digalactosyldiglyceride (DGDG) content in the N-deficient culture on day 29 was higher compared to the cells grown in N-rich media. Increased DGDG content upon N-deprivation has also been reported for two cyanobacteria, *Pseudanabaena* sp. and *Oscillatoria splendida*, due to an increase in mainly palmitic (16:0) and linolenic acid (18:3; de Loura et al. 1987).

The relative distribution of *C. sorokiniana* acyl hydrocarbons, measured as fatty acid methyl esters (GC/MS) is shown in Fig. 4 and Table 2. All lipids show carbon number and acyl double bond distributions that reflect the predominance of C14–C18 acyl hydrocarbons with 0–3 double bonds per acyl unit. The C16:0, C16:2, C18:2, and C18:3 fatty acids being most abundant. In particular, the omega-3 fatty acid C18:3 is the most abundant acyl moiety for all time points and ranges from 26 to 48 % of the total acyl hydrocarbon content. Consistent with the previous studies, linolenic acid increased under N deprivation (Li et al. 2013; Fig. 4), whereas under unstressed conditions there were higher levels of more saturated 18:1 and 18:2 fatty acids in *C. sorokiniana* UTEX 1230 (Rosenberg et al. 2014).

Finally, total energy content of the cells was determined by calorimetry for each time point. As expected, N-depleted cells had 29 % (day 18) and 38 % (day 29) higher energy density relative to N-replete cells which is consistent with increased lipid content (Fig. 5). Between day 18 and day 29, the total

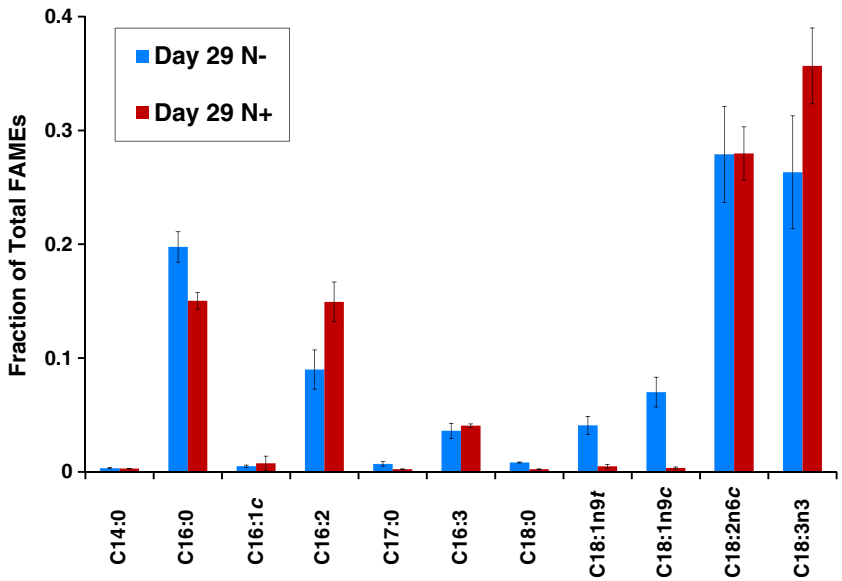

Fig. 4 Acyl-hydrocarbon distribution determined by base-catalyzed GC/MS FAME analysis of *C. sorokiniana* cultures

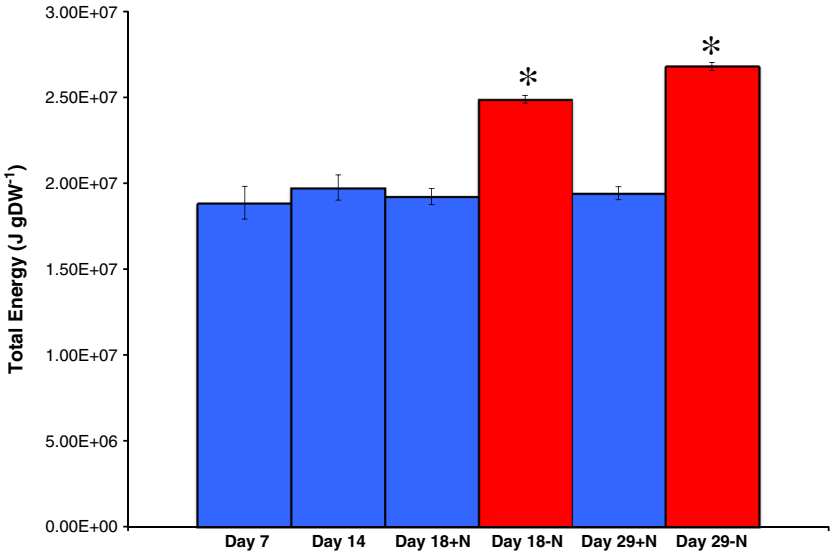

Fig. 5 Calorimetric analysis and energy density (calories per gram dry weight) of nitrogen-replete (+N) and nitrogen-deplete (−N) cells. Results represent the average and SE of three independent measurements. *Asterisk* represents statistically significant differences at $P=0.05$

energy in N-depleted cells increased by 64 % (Supplemental Figure 4), associated with the formation of TAGs.

In conclusion, it was demonstrated that TAGs increased 20-fold, and energy density increased by 64 % over the 1 month time course of the experiment for cells grown under N-deplete conditions relative to cultures grown in the presence of N. At the same time N depletion had less impact on total cell numbers or biomass yield. Regardless, the increases in energy density coupled with the differences in biomass yield between N-deplete and N-replete cultures resulted in a total energy yield of 23.6×10^6 J for the N-deplete and 14.4×10^6 J for the N-replete culture or a 1.6-fold greater total energy yield for the N-deplete culture (Supplemental Figure 4). To support this additional energy accumulation would require a greater total net culture photosynthetic rate or a reduced loss of previously fixed carbon through respiration or secretion of organic compounds. The small changes in respirations rates observed could not account for the increase in energy yield in N-deplete cultures. It is proposed that the enhanced total energy yield in N-deplete cultures relative to N-replete cultures could only be accounted for by greater net culture photosynthesis associated with reduced self-shading and enhanced light penetration. The increase in lipid yield is associated with reductions in some plastid lipids but not others. At present, it is unclear if lipid remodeling contributes substantially to increases in TAG content. Regardless, N limitation does lead to enhanced TAG accumulation and energy density in *C. sorokiniana*. The elimination of N from the media has other practical implications; inoculation with cells having sufficient N for a complete grow out period in media lacking N is likely to reduce competition by weedy algae, allowing for enhanced cultivation management and yield potential.

Acknowledgments We thank Paige Pardington for her help in assisting with the photobioreactors during this experiment. This work is supported by the U.S. Department of Energy under contract DE-EE0003046 awarded to the National Alliance for Advanced Biofuels and Bioproducts for RTS and TS and by the Center for Animal Health and Food Safety at New Mexico State University for TS.

References

Berges JA, Charlebois DO, Mauzerall DC, Falkowski PG (1996) Differential effects of nitrogen limitation on photosynthetic efficiency of photosystems I and II in microalgae. Plant Physiol 110:689–696

Breuer G, Lamers PP, Martens DE, Draaisma RB, Wijffels RH (2012) The impact of nitrogen starvation on the dynamics of triacylglycerol accumulation in nine microalgae strains. Bioresour Technol 124: 217–226

Cakmak T, Angun P, Demiray YE, Ozkan AD, Elibol Z, Tekinay T (2012) Differential effects of nitrogen and sulfur deprivation on growth and biodiesel feedstock production of *Chlamydomonas reinhardtii*. Biotechnol Bioeng 109:1947–1957

Carvalho AP, Silva SO, Baptista JM, Malcata FX (2011) Light requirements in microalgal photobioreactors: an overview of biophotonic aspects. Appl Microbiol Biotechnol 89:1275–1288

de Loura IC, Dubacq JP, Thomas JC (1987) The effects of nitrogen deficiency on pigments and lipids of cyanobacteria. Plant Physiol 83:838–843

Folch J, Lees M, Sloane Stanley GH (1957) A simple method for the isolation and purification of total lipides from animal tissues. J Biol Chem 226:497–509

Holguin F, Schaub T (2013) Characterization of microalgal lipid feedstocks by direct infusion FT-ICR mass spectrometry. Algal Res 2: 43–50

Huerlimann R, de Nys R, Heimann K (2010) Growth, lipid content, productivity, and fatty acid composition of tropical microalgae for scale-up production. Biotechnol Bioeng 107:245–257

Li T, Zheng Y, Yu L, Chen S (2013) High productivity cultivation of a heat-resistant microalga Chlorella sorokiniana for biofuel production. Bioresour Technol 131:60–67

Lizzul AM, Hellier P, Purton S, Baganz F, Ladommatos N, Campos L (2014) Combined remediation and lipid production using *Chlorella sorokiniana* grown on wastewater and exhaust gases. Bioresour Technol 151:12–18

Lourenco SO, Barbarino E (1998) Distribution of intrecellular nitrogen in marine microalgae: basis for the calculation of specific nitrogen-to-protein conversion factors. J Phycol 34:798–811

Lu C, Zhang J, Zhang Q, Li L, Kuang T (2001) Modification of photosystem II photochemistry in nitrogen deficient maize and wheat proteins. J Plant Physiol 158:1423–1430

Lv JM, Cheng LH, Xu XH, Zhang L, Chen HL (2010) Enhanced lipid production of *Chlorella vulgaris* by adjustment of cultivation conditions. Bioresour Technol 101:6797–6804

Mackinney G (1941) Absorption of light by chlorophyll solutions. J Biol Chem 140:315–322

Mata TM, Martins AA, Caetano NS (2010) Microalgae for biodiesel production and other applications: a review. Bioresour Technol 131:60–67

Murphy TE, Berberoglu H (2012) Effect of algae pigmentation on photobioreactor productivity and scale-up: a light transfer perspective. J Quant Spectrosc Radiat Transf 112:2826–2834

Neidhardt J, Benemann JR, Zhang L, Melis A (1998) Photosystem-II repair and chloroplast recovery from irradiance stress: relationship between chronic photoinhibition, light-harvesting chlorophyll antenna size and photosynthetic productivity in *Dunaliella salina* (green algae). Photosynth Res 56:175–184

Perrine Z, Negi S, Sayre RT (2012) Optimization of photosynthetic light energy utilization by microalgae. Algal Res 1:134–142

Pruvost J, Van Vooren G, Le Gouic B, Couzinet-Mossion A, Legrand J (2011) Systematic investigation of biomass and lipid productivity by microalgae in photobioreactors for biodiesel application. Bioresour Technol 102:150–158

Ramanna L, Guldhe A, Rawat I, Bux F (2014) The optimization of biomass and lipid yields of Chlorella sorokiniana when using wastewater supplemented with different nitrogen sources. Bioresour Technol 168:127–135

Rosenberg JN, Kobayashi N, Barnes A, Noel EA, Betenbaugh MJ, Oyler GA (2014) Comparative analyses of three *Chlorella* species in response to light and sugar reveal distinctive lipid accumulation patterns in the microalga *C. sorokinian*a. PLoS One 9:e92460

Sayed OH, Hegazy AK (1992) Inhibition of secondary carotenoid biosynthesis during degreening of *Chlorella fusca* (Chlorococcales, Chlorophyta) and implication for growth and survival. Cryptogam Algol 13:181–186

Sayre RT (2010) Microalgal biofuels; carbon capture and sequestration. Bioscience 60:722–727

Sharma KK, Schuhmann H, Schenk PM (2012) High lipid induction in microalgae for biodiesel production. Energies 5:1532–1553

Siaut M, Cuine S, Cagnon C, Fessler B, Nguyen M, Carrier P, Beyly A, Beisson F, Triantaphylides C, Li-Beisson Y, Peltier G (2011) Oil accumulation in the model green alga *Chlamydomonas reinhardtii*: characterization, variability between common laboratory strains and relationship with starch reserves. BMC Biotechnol 11:1–15

Simionato D, Block MA, La Rocca N, Jouhet J, Marechal E, Finazzi G, Morosinotto T (2013) Response of *Nannochloropsis gaditana* to nitrogen starvation includes a de novo biosynthesis of triacylglycerols, a decrease of chloroplast galactolipids and a reorganization of the photosynthetic apparatus. Eukaryot Cell 12:665–676

Spolaore P, Joannis-Cassan C, Duran E, Isambert A (2006) Commercial applications of microalgae. J Biosci Bioeng 101:87–96

Subramanian S, Barry AN, Pieris S, Sayre RT (2013) Comparative energetics and kinetics of autotrophic lipid and starch metabolism in chlorophytic microalgae: implications for biomass and biofuel production. Biotechnol Biofuels 6:150–162

Sueoka N (1960) Mitotic replication of deoxyribonucleic acid in *Chlamydomonas reinhardi*. Proc Natl Acad Sci 46:83–91

Tamburic B, Guruprasad S, Radford DT, Szabo M, Lilley RM, Larkum AW, Franklin JB, Kramer DM, Blackburn SI, Raven JA, Schliep M, Ralph PJ (2014) The effect of diel temperature and light cycles on the growth of *Nannochloropsis oculata* in a photobioreactor matrix. PLoS One 9:e86047

Tang H, Chen M, Garcia ME, Abunasser N, Ng KY, Salley SO (2011) Culture of microalgae *Chlorella minutissima* for biodiesel feedstock production. Biotechnol Bioeng 108:2280–2287

Wang S-T, Pan Y-Y, Liu C-C, Chuang L-T, Chen C-NN (2011) Characterization of a green microalga UTEX 2219–4: effects of photosynthesis and osmotic stress on oil body formation. Bot Stud 52:305–312

Zhang YM, Chen H, He CL, Wang Q (2013) Nitrogen starvation induced oxidative stress in an oil-producing green alga *Chlorella sorokiniana* C3. PLoS One 8:e69225